

3D FINITE ELEMENT SIMULATIONS OF REINFORCED CONCRETE ELEMENTS EXPOSED TO FIRE

Erol Lale*, Chiara Ceccato†

* Department of Civil Engineering
Istanbul Technical University
34469 Maslak Istanbul, Turkey
e-mail: lale@itu.edu.tr

†Dept. of Civil and Environmental Engineering
Hong Kong Polytechnic Univ., Hong Kong, China
e-mail: chiara.ceccato@polyu.edu.hk

Key words: Fire, concrete, transient creep, damage-plasticity, finite elements

Abstract. Fire could dramatically reduce strength of reinforced concrete elements and it is considered one of the major threats for the structural safety of buildings: structural members may even collapse due to intensity and duration of fire. In this study, 3D finite element simulations of reinforced concrete elements under fire loading are presented. A quasi static one-way-coupled thermo-mechanical analysis is carried out, in which a heat transfer simulation is conducted first and then internal forces are computed. A phenomenological constitutive model based on damage-plasticity is used for concrete at high temperature. Transient creep strains are included in the model for elevated temperature. Extended Leon model is used for yield function and isotropic damage is assumed. Numerical results are compared with experimental data found in the literature, showing good agreement.

1 INTRODUCTION

Concrete, as one of the most widely used construction material, is likely exposed to high temperature, in case of extreme events such as explosions and during fire or in special structures such as nuclear vessels. Its mechanical properties, like density, thermal expansion, and thermal conductivity, require a careful evaluation in order for the material performance to be understood under extreme high temperature. In general, strength and stiffness of concrete decrease with the increase of temperature and degradation of concrete mechanical behaviors mainly results from dehydration of concrete at the micro-level [1]. The behavior of concrete though is particularly complex to predict, due to the differences of each constitution in terms of thermal response, with several factors affecting the fire resistance (eg. concrete strength, moisture content, concrete density, aggregate type). For example, high strength concrete (HSC) has lower permeability and water-cement

ratio than normal strength concrete (NSC), therefore, under high temperature exposure, moisture can escape with a slower rate, leading to a faster increase in pore pressure and consequently a major reduction in load bearing capacity [2]. Thus, fire design and assessment of structure has become a fundamental aspect of structural design and, in this contest, urges the development of computational models capable of accurately capturing the behavior of reinforced concrete elements at elevated temperatures.

In this study, a plastic damage model for the simulation of concrete behavior under elevated temperature has been developed. The constitutive model adopted is based on isotropic damage coupled with plasticity in effective stress space. While hardening under compressive loading is modeled within the plasticity framework, softening under both tensile and compressive loadings are taken into account within the damage mechanics framework, where damage is modeled as a function of plastic strains. A sequential coupled thermo-mechanical analysis has been chosen: firstly, a transient heat transfer analysis is carried out to determine the temperature distribution over the specimen; then, based on its results, a mechanical analysis is conducted. For thermal analysis, material parameters such as specific heat, thermal conductivity coefficient are taken from standard design codes or experimental studies found in literature such as [3, 1]. Moisture diffusion and phase change during elevated temperatures are not considered at this stage.

2 Constitutive Model

The total strain tensor can be decomposed into mechanical strain ϵ_σ , free thermal strain ϵ_{fth} , creep strain ϵ_{cr} , and transient creep strain ϵ_{tcr} , as shown below:

$$\epsilon_{total} = \epsilon_\sigma + \epsilon_{fth} + \epsilon_{cr} + \epsilon_{tcr} \quad (1)$$

Generally, the creep strain is considerably smaller than the other strain components in fire applications, due to the short duration of a fire events and, therefore, it can be neglected for fire safety assessment of structures [4].

2.1 Constitutive Model at ambitious temperature

According to incremental theory of plasticity, the mechanical strain tensor ϵ_σ can be split into elastic ϵ^e and plastic components, ϵ^p :

$$\epsilon_\sigma = \epsilon_e + \epsilon_p \quad (2)$$

The elastic part is the recoverable portion of the total strain and, considering linear elasticity, it is given by

$$\epsilon_e = D^{-1}\sigma \quad (3)$$

where D and σ are the elasticity tensor and the stress tensor respectively. By using these two equations, stress relation with strain can be defined as:

$$\sigma = D(\epsilon - \epsilon_p) \quad (4)$$

If we assume that the stiffness degradation is isotropic (scalar), then the stiffness tensor is written as:

$$D = (1 - \omega) D^e \quad (5)$$

where ω is the damage parameter and D^e is the initial elasticity tensor. Substitution of equation (4) into (3) leads to the following equation:

$$\sigma = (1 - \omega) D^e (\epsilon - \epsilon_p) = (1 - \omega) \bar{\sigma} \quad (6)$$

where $\bar{\sigma}$ is the effective stress, defined as:

$$\bar{\sigma} = D^e (\epsilon - \epsilon_p) \quad (7)$$

According to this equation, the constitutive relation for the damage response can be decoupled from the plastic response, providing numerical advantages.

Several combined plasticity and damage models have been developed in recent years. To ensure that a constitutive model remains thermodynamically admissible, the second principle of thermodynamics must be satisfied, which requires non-negative dissipation and this condition leads to certain constraints on the constitutive model. Grassl and Jirasek [5] studied thermodynamic admissibility of different types of coupling of damage and plasticity and have shown that, formulating the plasticity constitutive model in terms of effective stress, the only condition required for the thermodynamic admissibility is the softening plastic modulus not to drop below a critical value, given by the pure plastic model.

2.1.1 Plasticity Formulation

In order to obtain the effective stress due to strain increment, the increase of plastic strain has to be estimated. Plasticity formulations require a yield function, a flow rule and a hardening rule:

$$\begin{aligned} f^p(\bar{\sigma}, \kappa_p) &\leq 0 \\ \dot{\epsilon}_p &= \dot{\lambda} \frac{\delta g^p}{\delta \bar{\sigma}} \\ \dot{\kappa}_p &= \dot{\lambda} H. \end{aligned} \quad (8)$$

The Kuhn-Tucker conditions for loading-unloading need to be satisfied: $f^p(\bar{\sigma}, \kappa_p) \leq 0, \dot{\lambda} \geq 0, \dot{\lambda} f^p(\bar{\sigma}, \kappa_p) = 0$. Here f^p and g^p denote the yield surface and the plastic potential function respectively, λ_p is the plastic multiplier, $\kappa_p = [\kappa_p^t, \kappa_p^c]$ is (accumulated plastic strains) plastic state variables, and H is the matrix for multiaxial stress situation:

$$H(\bar{\sigma}, \epsilon^p) = \begin{bmatrix} \chi(\hat{\bar{\sigma}}) & 0 & 0 \\ 0 & 0 & -(1 - \chi(\hat{\bar{\sigma}})) \end{bmatrix} \frac{\delta g^p}{\delta \hat{\bar{\sigma}}} \quad (9)$$

where $\hat{\sigma}$ denotes the principal effective stress and χ is a weight factor defined as [6] :

$$\chi = \frac{\sum_{i=1}^3 \langle \hat{\sigma} \rangle}{\sum_{i=1}^3 |\hat{\sigma}|} \quad (10)$$

The extended Leon Model, successfully used for the simulation of the concrete behavior under uniaxial, biaxial and multi-axial loadings by many researchers [7, 8, 5, 9], is employed in this study for the definition of the yield surface, which is smooth and convex except for the point where parabolic meridians intersect the hydrostatic axis. The yield function is given in terms of invariant of effective stress tensor, hardening parameter, k and friction parameter, m_0 as follows:

$$f^p = \left[(1-k) \left(\frac{\bar{p}}{f_c} + \frac{\bar{\rho}}{\sqrt{6}f_c} \right)^2 + \sqrt{\frac{3}{2}} \frac{\bar{\rho}}{f_c} \right]^2 + k^2 m_0 \left(\frac{\bar{p}}{f_c} + \frac{\bar{\rho} r(\theta)}{\sqrt{6}f_c} \right) - k^2 = 0 \quad (11)$$

where $\bar{p} = \bar{I}_1/3$, $\bar{\rho} = \sqrt{2\bar{J}_2}$, $\theta = \cos^{-1} \left(3\sqrt{3}/2\bar{J}_3/\bar{J}_2^{3/2} \right) / 3$ denote the effective mean stress, the deviatoric radius and the Lode angle respectively and \bar{I}_1 is the first invariant of stress tensor, \bar{J}_2 , \bar{J}_3 are the second and the third invariant of deviatoric stress tensor. The friction parameter depends on compressive and tensile strength of concrete and it is given by:

$$m_0 = 3 \frac{f_c^2 - f_t^2}{f_c f_t} \frac{e}{e+1} \quad (12)$$

The shape of the deviatoric section is controlled by the function, $r(\theta, e)$,

$$r(\theta) = \frac{4(1-e^2)\cos^2\theta + (2e-1)^2}{2(1-e^2)\cos(\theta) + (2e-1)\sqrt{4(1-e^2)\cos^2(\theta) + 5e^2 - 4e}} \quad (13)$$

where e is the eccentricity parameter, calibrated according to the biaxial strength of concrete.

A non-associated flow rule is adopted in order to control excessive dilatancy, which is necessary to guarantee a realistic modeling of cohesive frictional material such as concrete and rocks. The plastic potential function controls the direction of the plastic strains and hence the relative ratios between the plastic strain components. The plastic potential is defined as follows;

$$g^p = \left[(1-k) \left(\frac{\bar{p}}{f_c} + \frac{\bar{\rho}}{\sqrt{6}f_c} \right)^2 + \sqrt{\frac{3}{2}} \frac{\bar{\rho}}{f_c} \right]^2 + k^2 \left(m_g \frac{\bar{p}}{f_c} + m_0 \frac{\bar{\rho}}{\sqrt{6}f_c} \right) - k^2 = 0 \quad (14)$$

where m_g is variable controlling the dilatation of concrete.

The non-linear behavior of concrete in the pre-peak region is described by isotropic hardening. The hardening parameter, $k = f_c/f_{cu}$, which controls the evolution of yield surface under compression, is defined in terms of equivalent plastic strain:

$$\begin{aligned}
 k &= k_0 + (1 - k_0) \sqrt{1 - \left(1 - \kappa_p^c / \kappa_p^{peak}\right)^2} & \text{for } \kappa_p^c \leq \kappa_p^{peak} \\
 k &= 1 & \text{for } \kappa_p^c > \kappa_p^{peak}
 \end{aligned} \tag{15}$$

$k_0 = f_{c0}/f_{cu}$ is the initial yield strength and κ_p^{peak} the plastic strain value at strength of concrete under uniaxial compression. Softening under compressive loading and tensile behavior is modeled with the damage formulation described in the session below.

2.1.2 Damage Formulation

Elastic stiffness degradation and softening under both compression and tension are formulated using an isotropic damage. Concrete behaves differently under tensile and compressive loading, therefore, two different damage formulations, one for tensile damage ω_t and one for compressive damage ω_c , are defined independently, following Lee and Fenves [6]. Damage is assumed to be depended on the accumulated plastic strain, hence no additional damage surface is required. Internal damage variables are defined equal to the plastic variables, i.e. $\kappa_d^t = \kappa_p^t$, $\kappa_d^c = \kappa_p^c$. Damage evolution law is assumed in the following exponential form:

$$\begin{aligned}
 \omega_t &= 1 - e^{-\kappa_d^t/a_t} \\
 \omega_c &= 1 - e^{-((\kappa_d^c - \bar{\epsilon}_0^p)/a_c)^2}
 \end{aligned} \tag{16}$$

Where a_t and a_c are material constant for tension and compression loading respectively to be calibrated against uniaxial test results. When tensile and compressive damage parameters are obtained, then the total damage is calculated as follows:

$$\omega = 1 - (1 - \omega_t)(1 - \omega_c) \tag{17}$$

3 EFFECTS OF TEMPERATURE ON MATERIAL CHARACTERISTICS

3.1 Free Thermal Strain

The free thermal strain of concrete depends on the type of aggregate used. Eurocode [10] suggests the following values for the free thermal strain.

For siliceous aggregates:

$$\begin{aligned}
 \epsilon_{th} &= -1.8 \times 10^{-4} + 9 \times 10^{-6}T + 2.3 \times 10^{-11}T^3 & \text{for } 20^\circ C \leq T \leq 700^\circ C \\
 \epsilon_{th} &= 14 \times 10^{-3} & \text{for } 700^\circ C < T \leq 1200^\circ C
 \end{aligned} \tag{18}$$

For calcareous aggregates:

$$\begin{aligned}
 \epsilon_{th} &= -1.2 \times 10^{-4} + 6 \times 10^{-6}T + 1.4 \times 10^{-11}T^3 & \text{for } 20^\circ C \leq T \leq 700^\circ C \\
 \epsilon_{th} &= 12 \times 10^{-3} & \text{for } 700^\circ C < T \leq 1200^\circ C
 \end{aligned} \tag{19}$$

In this study, the free thermal strain increment is calculated as follows:

$$\dot{\epsilon}_{fth} = \alpha \dot{T} \mathbf{I} \quad (20)$$

where \mathbf{I} denotes the second order identity matrix and α the coefficient of free thermal strain which can be obtained from the free thermal strain given by Eurocode. Also Nielsen et al. [11] suggested the following function for coefficient of free thermal strain:

$$\begin{aligned} \alpha &= 6 \times 10^{-5} / (7 - \bar{\theta}) \quad \text{for } 0 \leq \bar{\theta} \leq 6 \\ \alpha &= 0 \quad \text{for } \bar{\theta} > 6 \end{aligned} \quad (21)$$

Here $\bar{\theta} = (T - 20) / 100$ represents the normalized temperature.

3.2 Transient creep

When concrete is first loaded and then heated, the thermal strain in the material is higher than that experienced by unloaded specimens. This strain difference is called transient creep strain or load induced thermal strain and an exhaustive overview of this phenomenon can be found in Torelli et. al [12]. The transient creep strain, which is an irreversible strains, depends on the temperature reached by the material and it is proportional to the compressive load level. Experimental results have shown that it does not depend on the heating rate or age of concrete [13]. Following De Borst and Peeters [14], it is modeled as follows:

$$\epsilon_{tr} = F_{tr} H_{tr} \frac{\sigma^-}{f_{c,T_0}} \quad (22)$$

where F_{tr} is the transient creep function, σ^- the negative part of effective stress tensors, f_{c,T_0} the concrete strength at ambient air temperature T_0 . H is a fourth order tensor defined as:

$$H_{tr} = -\nu_{tr} \delta_{ij} \delta_{kl} + \frac{1}{2} (1 + \nu_{tr}) (\delta_{ik} \delta_{jl} + \delta_{il} \delta_{jk}) \quad (23)$$

Here ν_{tr} is the Poisson ratio for transient creep components. F_{tr} denotes the change of transient creep strain with respect to temperature under uniaxial loading and its function has been described by several different models in the literature. In particular, Pearce et al. [15] have given the following parabolic function:

$$\begin{aligned} F_{tr} &= 0.01 \times (2A\bar{\theta} + B) \quad \text{for } 0 \leq \bar{\theta} \leq \bar{\theta}^* \\ F_{tr} &= 0.01 \times [2C(\bar{\theta} - \bar{\theta}^*) + 2A\bar{\theta}^* + B] \quad \text{for } \bar{\theta} > \bar{\theta}^* \end{aligned} \quad (24)$$

$\bar{\theta}^* = 4.5$, $A = 4 - 6\%$, $B = 1 - 1.5\%$ and $C = 7 - 10\%$ values are suggested in the same paper.

3.3 Compressive behavior of Concrete exposed to elevated temperature

The temperature dependency of concrete compressive strength is taken from Eurocode 2. Eurocode provides tabular data for siliceous and calcareous aggregates concrete, which can be approximated by the exponential curve given below:

$$\begin{aligned} f'_{c,T} &= f'_{c,0} \exp [-(\bar{T}/5.5)^2] && \text{for siliceous aggregate} \\ f'_{c,T} &= f'_{c,0} \exp [-(\bar{T}/5.5)^{2.5}] && \text{for calcareous aggregate} \end{aligned} \quad (25)$$

where $\bar{T} = (T - 100) / 100$ is the relative temperature.

The ratio of tensile and compressive strength is assumed constant, i.e. degradation of tensile strength is assumed to be equal compressive one.

3.4 Modulus of Elasticity

The modulus of elasticity is assumed to be a function of temperature and the formulation given by Stabler [16] is adopted in this study, as follows:

$$E_c(T) = (1 - \omega_E) E(T_0) \quad (26)$$

where ω_E denotes thermal degradation of Modulus of elasticity and it is formulated as :

$$\begin{aligned} \omega_E &= 0.2\bar{T} - 0.01\bar{T}^2 && \text{for } 0 \leq \bar{T} \leq 10 \\ \omega_E &= 1.0 && \text{for } \bar{T} > 10 \end{aligned} \quad (27)$$

where $\bar{T} = (T - T_0) / 100$ is relative temperature and $T_0 = 20$ °C.

4 NUMERICAL RESULTS

4.1 Transient creep model

Firstly, an axially restrained cubic specimen is simulated in order to check the implementation of the transient creep formulation. For this simulation, the material parameters have been assumed following Torelli et. al [12]: $\nu_{tr} = 0.37$, $E = 47000$ MPa (Elastic Modulus), $\nu = 0.2$ (Poisson ratio), $f_{cu} = 57$ MPa (compressive strength), $f_t = 5.7$ MPa (tensile strength). The specimen is exposed to heating-cooling cycles up to 140 °C and 180 °C and then it is heated up to 220 °.

The numerical results in terms of temperature vs stress curves are shown in figure 1. As soon as the temperature increases, compressive stresses occur in the material, due to the prevented thermal expansion, causing transient creep strain. With the increase of transient creep strain, a stress relaxation is observed, which is the reason for the reduction of stress with the increase of temperature. During the cooling phase, the transient creep strain does not change and does not increase until the temperature values reach the maximum value experienced during the temperature history.

The experimental tests conducted by Anderberg and Thelandersson [17] are simulated to validate the transient creep model. The concrete specimen was loaded first and then heated up a certain temperature level. In particular, the specimen was subjected to different levels of compression: $\zeta = 0$, $\zeta = 0.225$, $\zeta = 0.35$, $\zeta = 0.45$ and $\zeta = 0.675$, with ζ being the ratio between the applied stress and the material strength. In this example,

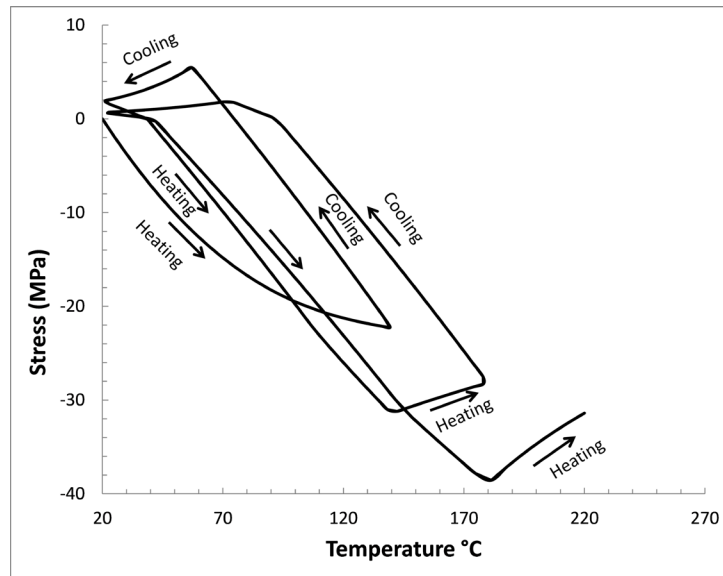


Figure 1: Uniaxially restrained specimen subjected to temperature cycle

the coefficient of free thermal strain is given in Eq. 21 and the following parameters for the transient creep function are adopted: $A = 0.004$, $B = 0.001$ and $C = 0.007$. The numerical results, plotted in Fig. 2, show a good agreement with the experimental data, confirming that the free thermal expansion is well captured by the model.

4.2 Reinforced concrete beam

After the validation of the transient creep model, a reinforced concrete beam has been simulated with the proposed model. A simply supported beam tested by Lin et. al [18] has been selected to compare with numerical results. The beam is characterized by a 6.1 m long span between supports and a 305×355 mm rectangular cross-section, reinforced with $4\phi 19$ rebars on the tension side and $2\phi 19$ rebars on the compression side. The compressive strength of concrete is $f_{cu} = 29.5$ MPa and yield strength of steel $f_y = 435.8$ MPa. The beam has been loaded up to certain level of load first and then exposed to ASTM E119 fire from three sides. The results of the heat transfer analysis are shown in Fig. 3, in terms of temperature vs. time for the corner rebar. Fig. 4 shows the mid-span deflection of the beam with respect to temperature and, numerical results are in good agreement with experimental ones, confirming the prediction capability of the present model.

5 CONCLUSION

In this study, a damage plasticity model for concrete under elevated temperature has been developed, where the transient creep strain are explicitly obtained. The performance of the model is validated by a comparison with experimental results gathered from the literature: the adopted model for transient creep model has been firstly validated for a concrete specimen and then a 3D reinforced concrete beam has been simulated with the proposed model. The results have shown good agreement, proving that the model can

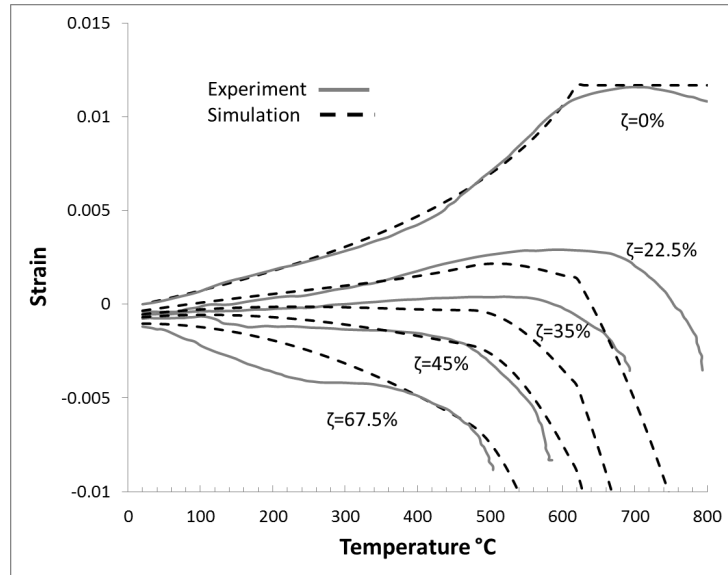


Figure 2: Strain upon heating under constant load levels

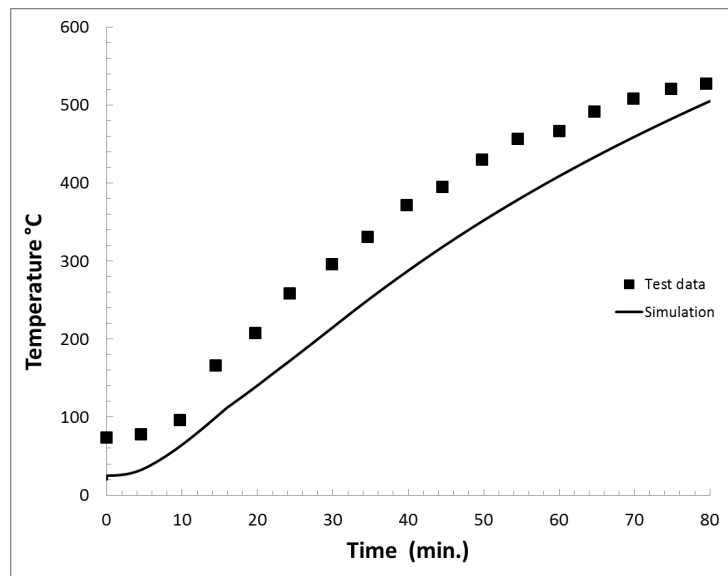


Figure 3: Evaluation of corner rebars temperature with time

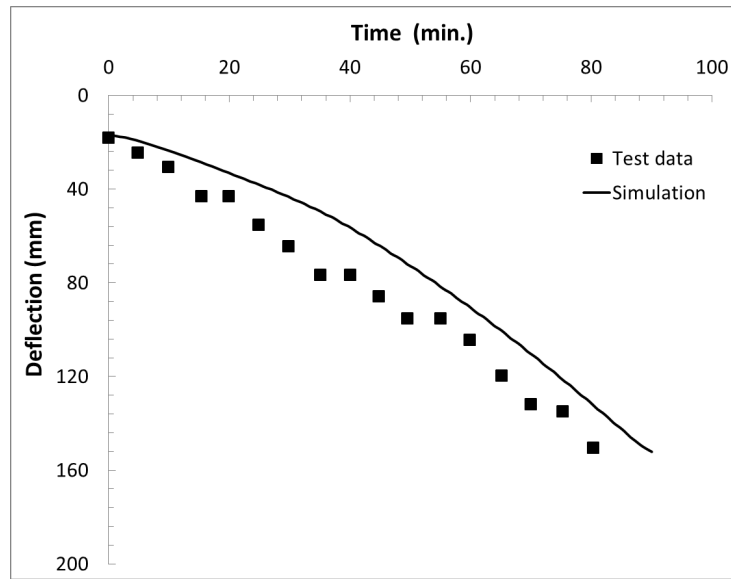


Figure 4: Mid-span deflection of the RC beam

capture the behavior of concrete expose to high temperatures.

In the experimental tests reported in literature, no significant spalling is observed for normal strenght concrete (NSC), but it becomes an important issues for high strength concrete (HSC) due to its low porosity [19]. Consequently, the moisture diffusion in the concrete and spalling will be introduced to model.

REFERENCES

- [1] V. Kodur, “Properties of concrete at elevated temperatures,” *ISRN Civil engineering*, vol. 2014, 2014.
- [2] V. Kodur, “fire performance of high-strength concrete structural members,” *Institute for Research in Construction*, 1999.
- [3] T. Harmathy, “Thermal properties of concrete at elevated temperatures,” *Journal of Materials*, 1970.
- [4] T. Gernay, A. Millard, and J.-M. Franssen, “A multiaxial constitutive model for concrete in the fire situation: Theoretical formulation,” *International Journal of Solids and Structures*, vol. 50, no. 22, pp. 3659–3673, 2013.
- [5] P. Grassl and M. Jirásek, “Damage-plastic model for concrete failure,” *International journal of solids and structures*, vol. 43, no. 22, pp. 7166–7196, 2006.
- [6] J. Lee and G. L. Fenves, “Plastic-damage model for cyclic loading of concrete structures,” *Journal of engineering mechanics*, vol. 124, no. 8, pp. 892–900, 1998.
- [7] G. Etse and K. Willam, “Fracture energy formulation for inelastic behavior of plain concrete,” *Journal of engineering mechanics*, vol. 120, no. 9, pp. 1983–2011, 1994.